Acta Pharmacologica Sinica

www.nature.com/aps

ARTICLE

OTUD1 positively regulates microglia neuroinflammation and promotes the pathogenesis of Alzheimer's disease by deubiquitinating C/EBPβ

Ling-yu She[1,2,3], Lu-yao Li[1], Hao Tang[1,3], Qin Yu[1], Feng-yi Gao[1], Yu-qing Zeng[1,2], Lin-jie Chen[1,2], Li Xiong[3], Li-wei Li[3], Fan Chen[1,3], Jin-feng Sun[1,4], Wen-hua Zheng[5], Xia Zhao[1,2,3]✉ and Guang Liang[1,2,3]✉

Alzheimer's disease (AD) is the most common neurodegenerative disease worldwide. Microglia-mediated neuroinflammation is closely associated with AD pathogenesis. Abnormal deubiquitinating enzyme (DUB) expression is associated with neuroinflammation. Identification of functional DUBs in microglia may provide novel targets for AD treatment. Here, we found that the levels of DUB, ovarian tumor deubiquitinase 1 (OTUD1), were upregulated in AD model mice and amyloid-beta-induced microglia. OTUD1 knockdown in microglia significantly inhibited neuroinflammation, thereby improving cognitive impairment in AD model mice. Liquid chromatography-tandem mass spectrometry analysis coupled with co-immunoprecipitation revealed the CCAAT/enhancer-binding protein β (C/EBPβ), a key transcription factor regulating microglial inflammation, as an OTUD1-interacting protein. Mechanistically, OTUD1 bound to C/EBPβ and maintained its stability by removing the K48 ubiquitin chain at K253 of C/EBPβ, thereby activating the C/EBPβ–nuclear factor-κB-mediated inflammatory responses in microglia. Overall, our results revealed the roles of the OTUD1–C/EBPβ axis in mediating the microglial inflammatory responses and AD pathology, facilitating the development of new strategies targeting microglial neuroinflammation for AD treatment.

Keywords: Alzheimer's disease; OTUD1; microglia; neuroinflammation; C/EBPβ

Acta Pharmacologica Sinica (2025) 0:1–14; https://doi.org/10.1038/s41401-025-01566-y

INTRODUCTION

Alzheimer's disease (AD) is a progressive neurodegenerative disease that impairs mental development and disrupts cognitive functions. It affects over 50 million people worldwide, posing a heavy burden on the affected patients and society [1, 2]. Currently, no effective treatment is available AD [3]. Microglia play critical roles in central nervous system development and brain homeostasis [4, 5]. Neuroinflammation is a pathological driver and important hallmark of AD pathogenesis. Activated microglia induce neuroinflammation and secrete proinflammatory factors, causing neuronal damage and promoting AD development [6]. Therefore, evaluation of microglial function regulation to combat neuroinflammation can facilitate the identification of novel targets and development of effective therapies for AD.

Ubiquitination, a reversible post-transcriptional modification of substrate proteins regulating the structure, stability, and functions of target proteins, is involved in the pathophysiological regulation of various. Deubiquitinases (DUBs) enzymatically reverse ubiquitination. To date, >107 DUBs involved in the regulation of various diseases have been identified in humans. Identification of functional DUBs in microglia may reveal novel targets for AD treatment. Ovarian tumor deubiquitinase 1 (OTUD1), a DUB belonging to the OTU protein family, is closely associated with immune and inflammatory responses in some non-neuron diseases [7–10]. OTUD1 knockout enhances the antiviral innate immune responses by increasing RIG-I-like receptor-mediated production of inflammatory cytokines and interferons [10]. We previously reported that OTUD1 knockout alleviates Ang II-induced renal and cardiac inflammation through deubiquitinating CDK9 and STAT3, respectively [11, 12]. However, to date, the specific roles of OTUD1 in microglia and inflammatory AD remain unknown.

In this study, we observed increased OTUD1 expression levels in the microglia of AD model mice and identified the key roles and action mechanisms of OTUD1 in microglia-mediated AD pathology. Microglia-specific OTUD1 knockdown significantly alleviated neuroinflammation and cognitive deficits in AD model mice. Mechanically, we found that OTUD1 interacted with and deubiquitinates CCAAT/enhancer-binding protein β (C/EBPβ), a key transcription factor regulating inflammation, to maintain its stability, thereby activating the C/EBPβ–nuclear factor (NF)-κB inflammatory signaling pathway in microglia. Overall, our results

[1]The First People's Hospital of Lin'an District, Affiliated Lin'an People's Hospital, Hangzhou Medical College, Hangzhou 310014, China; [2]Department of Pharmacy and Institute of Inflammation, Zhejiang Provincial People's Hospital, Affiliated People's Hospital, Hangzhou Medical College, Hangzhou 310014, China; [3]School of Pharmaceutical Sciences, Hangzhou Medical College, Hangzhou 311399, China; [4]Key Laboratory of Natural Medicines of the Changbai Mountain, Ministry of Education, Yanbian University, Yanji 133002, China and [5]Center of Reproduction, Development and Aging and Institute of Translation Medicine, Faculty of Health Sciences, University of Macau, Taipa, Macau 999078, China
Correspondence: Xia Zhao (xiazhao@hmc.edu.cn) or Guang Liang (wzmcliangguang@163.com)
These authors contributed equally: Ling-yu She, Lu-yao Li, Hao Tang

Received: 11 November 2024 Accepted: 10 April 2025
Published online: 07 May 2025

revealed the involvement of a new OTUD1–C/EBPβ axis in microglial activation and identified OTUD1 as a potential target for AD treatment.

MATERIALS AND METHODS

General reagents

Amyloid beta (Aβ)-peptide 1-42 (PA4391) was purchased from Ontores Biotechnologies, and the specific details are provided in Table S1. Flag-OTUD1, Flag, HA, His-C/EBPβ, HA-C/EBPβ, HA-Ub, HA-K48, and HA-K63 plasmids were obtained from Tsingke Biotech (Beijing, China). Lipofectamine 3000 (L3000-015; Thermo Fisher, MA, USA). Dulbecco's modified Eagle's medium (D0822) and dimethyl sulfoxide (DMSO; D2650) were purchased from Sigma (St. Louis, MO, USA). Additionally, FD Rapid Golgi Stain (PK401; FD Neuro Technologies), mouse Aβ42 ELISA (EM0864; Fine Test), mouse Aβ40 ELISA (EM0863; Fine Test) kits were purchased. Fetal bovine serum and 0.25% trypsin were purchased from Life Technologies (Grand Island, NY, USA) and Calbiochem (San Diego, CA, USA). Western Blot Marker (C520010) was purchased from Sangon Biotech (Shanghai, China). ECL (P10300) was obtained from NCM Biotech (Suzhou, China), and polyvinylidene fluoride membranes (1620177) were purchased from Bio-Rad. The Hifair III 1st Strand cDNA Synthesis SuperMix for qPCR (gDNA Digester Plus) kit (Cat. no. 11141ES60) was obtained from Yeasen. Phosphatase inhibitor cocktail (MCE; HY-K0010/HY-K0021), Pierce BCA Protein Assay Kit (23227; Thermo Fisher Scientific), and Pierce Classic Magnetic IP/Co-IP Kit (88804; Thermo Scientific) were also obtained. Quantitative polymerase chain reaction (qPCR) was performed using the SYBR Green kit (Cat. no. 11201ES08; Yeasen). Penicillin/streptomycin (Carlsbad, CA, USA) was also used. Small interfering RNA (siRNA) was purchased from GenePharma (Shanghai, China), and specific sequence information is shown in Table S1. All antibodies used and their sources are listed in Table S2.

Animals and treatment

Two AD models were used in this study: Aβ-infused OTUD1 knockout and 3×Tg mouse models with the specific knockout of OTUD1 in microglia. Eight-month-old APP Swedish, MAPT P301L, and PSEN1 M146V (3×Tg) and 8-month-old APP/PS1 (APPswe/PSEN1dE9) mice were purchased from Jackson Laboratory [13, 14] and raised in the Animal Laboratory of Hangzhou Medical College. These mouse models are commonly used in AD research [15, 16]. OTUD1$^{-/-}$ mice with a C57BL/6 J background were provided by Professor Fu-ping You at Peking University [11, 17]. All animals were housed in a room at 24–26 °C under, a 12/12-h light/dark cycle and provided *ad libitum* access to food and water. Age-matched female littermates were included in this study [18, 19].

(1) To study OTUD1 in microglia more specifically, we deliberately knocked out OTUD1 in the microglia of 3×Tg mice. We commissioned BrainVTA (Wuhan, China) to construct AAV vectors (AAV-shOTUD1:rAAV-CX3CR1-DIO-mCherry-5′miR30-shRNA(OTUD1)-3′miR30-WPRE plus Cre AAV (rAAV-CX3CR1-CRE-WPRE-hGH pA) that can specifically knockdown microglia OTUD1. The 3×Tg and wild-type (WT) mice were randomly divided into three groups: WT-AAV-NC (WT mice infused with AAV-NC; $n = 10$), 3×Tg-AAV-NC (3×Tg mice infused with AAV-NC; $n = 10$), and 3×Tg-AAV-shOTUD1 (3×Tg mice infused with AAV-shOTUD1; $n = 10$) groups. AAV-shOTUD1 or AAV-NC was microinjected into the bilateral hippocampus of 3×Tg-AD and WT mice. The coordinates were at bregma value 0, posterior opening was 2.0 mm, lateral opening was ±1.5 mm, and depth was 1.5 mm. Behavioral testing was performed after four weeks.

(2) Aβ-infused AD model was generated as previously described [16]. Eight-week-old C57BL/6 (WT) and OTUD1$^{-/-}$ on WT background mice were randomly divided into four groups: WT (WT mouse control; $n = 10$), Aβ (Aβ-infused WT mice; $n = 10$), OTUD1$^{-/-}$ (OTUD1$^{-/-}$ mouse control; $n = 10$), and OTUD1$^{-/-}$-Aβ (Aβ-infused OTUD1$^{-/-}$ mice; $n = 10$) groups. After anesthetizing the mice, Aβ (total 10 μg in 2 μL) or an equivalent amount of DMSO was injected. The needle was held in place for another 2 min and slowly withdrawn afterward.

Morris water maze (MWM) test

Briefly, on d 1–4 of the MWM test, a hidden platform was placed in the middle of one quadrant, approximately 1 cm below the water surface, and the mice were subjected to the hidden platform test to explore the time at which the mice found the hidden platform. On the fifth day after the start of the experiment, the hidden platform was removed and the mice were allowed to move freely for 60 s to conduct a space exploration test. Data acquisition and processing were performed using the MWM image automatic monitoring and processing system (VisuTrack, Shanghai, China).

New object recognition test (NORT)

NORT was used to test the recognition and memory abilities of mice. On the first day of the experiment, each mouse was allowed 5 min to explore two identical circular objects. On the second day, a round object was replaced with a square object, and each mouse still had only 5 min of exploration time, and the time and times of exploration of the two objects by the mouse were recorded.

Tissue samples preparation

After performing behavioral tests, the mice were sacrificed under deep anesthesia. Hydrolytic chloride (0.25 mg/mL) was used to euthanize all mice. In some mice, the brain was fixed with 4% paraformaldehyde for 24 h, dehydrated, embedded with OCT, and stored under −80 °C until further analysis. Brain tissue of another mouse was stored at −80 °C until use.

Golgi staining

After the mice were deeply anesthetized, the hippocampus from the mouse brain tissues was dissected, followed by Golgi staining using the FD Fast Golgi Staining Kit, according to the manufacturer's protocol. Brain tissues were immersed in a solution containing A and B and stored in the dark at room temperature for two weeks. After 24 h, the tissues were transferred to solution C and incubated in the dark at room temperature for one week. The solution was replaced after 24 h. The tissues were sliced into 100–200 μm thick slices using a cryoslicer at −20 °C. The slices were placed in a staining solution for 10 min and dehydrated in 50%, 75%, and 95% ethanol. The slices were made transparent with xylene and sealed with resin. Finally, images were acquired using a laser-scanning confocal microscope.

Immunofluorescence (IF) and Immunocytochemistry (ICC)

For IF, brain tissues were cut into 20 μm sections, permeabilized with 0.3% Triton X-100 for 20 min, blocked with 10% bovine serum albumin (BSA) solution for 1 h, and incubated with specific primary antibodies overnight at 4 °C. The next day, they were incubated with fluorophore-conjugated secondary antibodies for 1 h, and mounted on slides with antifade mountant containing 4′,6-diamidino-2-phenylindole.

For ICC, the cells were seeded in a glass-bottom dish, pretreated, fixed with 4% paraformaldehyde for 15 min, incubated with 0.3% Triton X-100 for 20 min, blocked with 10% BSA at room temperature for 1 h, and incubated again with specific primary antibodies overnight at 4 °C. The next day, the cells were incubated with fluorophore-conjugated secondary antibodies for 2 h. Then, a drop of the antifade mounting medium containing DAPI was added to stain the nuclei. Finally, images were captured using the Nikon A1 confocal microscope.

Cell culture and transfection
Mouse microglia (BV2, #SNL-155), rat pheochromocytoma cells (PC12 cells; #SNL-124), and mouse embryonic fibroblast (NIH3T3; #SNL-025) were obtained from the SUNNCELL (Wuhan, China). The cells were cultured in high-glucose Dulbecco's modified Eagle's medium, supplemented with 10% fetal bovine serum, 100 μg/mL streptomycin, and 100 units/ml penicillin and maintained at 37 °C in a humidified atmosphere of 5% CO_2. Then the cells were transfected with siRNA or expression plasmids using Lipofectamine 3000 according to the manufacturer's protocol.

Co-immunoprecipitation (Co-IP) and Western blotting
For Co-IP, protein concentrations were determined using BCA after total protein extraction. The Classic magnetic IP/Co-IP Kit was used in this test. Briefly, lysates were immunoprecipitated using the corresponding antibodies in the presence of Protein A + G Agarose, followed by Western blotting analysis.

Total protein was extracted from the cells or brain tissues using the radioimmunoprecipitation assay lysis buffer. Proteins were separated via 10% sodium dodecyl sulfate-polyacrylamide gel electrophoresis and transferred to polyvinylidene fluoride membranes. The membranes were blocked in 5% BSA for 1 h at room temperature and incubated overnight at 4 °C with specific primary antibodies. Protein bands were detected after incubation with horseradish peroxidase-conjugated secondary antibodies and enhanced chemiluminescence reagent. Band densities were quantified using the ImageJ software and normalized to the loading controls.

RNA isolation and quantitative real-time PCR
Total RNA was isolated from cultured cells using TRIZOL reagent according to the manufacturer's instructions. For RT-PCR analysis, cDNA was generated using the PrimeScript RT kit. Real-time PCR was performed using the CFX96 Touch Real-Time PCR Detection System (Bio-Rad) using TB Green Premix Ex Taq II. Relative expression was calculated by the $2^{-\Delta\Delta Ct}$ method and normalized to GAPDH. The primer sequences are shown in Table S1.

Enzyme-linked immunosorbent assay (ELISA)
Protein levels of interleukin (IL)-1β and tumor necrosis factor (TNF)-α in the supernatants of BV2 cultures were measured using ELISA kits (abs520001 and abs520010, respectively), following the manufacturer's instructions. Briefly, sample and test solutions were added to 96-well plates, gently mixed, and incubated at 37 °C for 60 min. After washing thrice, horseradish peroxidase conjugate was added, and the solutions were incubated at 37 °C for 20 min. Substrate solution was added and incubated in the dark at 37 °C for 30 min. Finally, termination solution was added to each well to stop the reaction. Optical density was measured at 450 nm within 5 min using a microplate reader. Data were quantitatively normalized to the protein concentrations in the control group.

Immunohistochemistry (IHC)
Paraffin-embedded brain tissues were cut into 5 μm-thick sections for histological analysis. The sections were dehydrated with graded concentrations of ethanol, and endogenous peroxidase activity was blocked with 3% (v/v) hydrogen peroxide in methanol for 10 min. Antigen retrieval was performed using 1 mM ethylenediaminetetraacetic acid buffer (pH 9.0) in a microwave. The cells were permeabilized with 0.5% Triton X-100 for 10 min and blocked with 10% BSA for 30 min. The sections were incubated overnight with specific primary antibodies. Then, 3,3′-diaminobenzidine color development was performed after incubation with the secondary antibodies. Finally, the sections were observed under a light microscope (Nikon, Japan).

Single-cell sequencing
Hippocampus from 3×Tg mouse brain tissue was collected, placed in a sterile RNase-free culture dish, and sent to LC-Bio Technology Co. LTD. (Hangzhou, China) in a tissue preservation solution for single-cell sequencing. Cell distribution of OTUD1 expression was analyzed using a cloud platform (https://www.omicstudio.cn/index). The dataset has been uploaded to the National Center for Biotechnology Information (accession number: BioProject PRJNA1230577).

Statistical analysis
Statistical analyses were performed using the GraphPad Prism 8 (GraphPad Software, San Diego, CA). Error bars represent the mean ± standard error of the mean. In the MWM test, escape latency times in the hidden platform trial were analyzed via two-way repeated measures analysis of variance. The statistical significance between multiple groups was determined using one-way ANOVA followed by Turkey's post-hoc test. Statistical significance was set at $p < 0.05$.

RESULTS

Microglial OTUD1 levels are upregulated in AD model mice
We first examined the correlation between OTUD1 and AD in using the hippocampal tissues of different AD mouse models. Protein levels of OTUD1 were significantly upregulated in these AD model mice, including APP/PS1, Aβ-infused, and 3×Tg mice (Fig. 1a–c). To determine the source of increased OTUD1 levels in glial cells, we performed double labeling with OTUD1 and a microglial marker (ionized calcium-binding adaptor molecule 1 [Iba1]) or an astrocyte marker (glial fibrillary acidic protein [GFAP]). Relative expression levels of OTUD1 were higher in microglia than in astrocytes, indicating microglia as the major glial cell types expressing OTUD1 (Fig. 1d). Next, we performed staining for Aβ, Iba1, and OTUD1 to examine the specific levels of OTUD1 in primary microglia in mice with or without AD. As shown in Fig. S1a, activated microglia in the vicinity of Aβ plaques exhibited upregulated levels of OTUD1 in 3×Tg AD model mice. Single-cell sequencing analysis of mouse hippocampal tissues identified 11 cell groups based on the marker gene levels in different cells (Fig. 1e). Gene mapping analysis revealed that OTUD1 is mainly expressed in microglia (Fig. 1f). We also examined the protein levels of OTUD1 in a cultured microglia BV2 cell line. OTUD1 levels were increased in time- and dose-dependent manners in BV2 cells after Aβ challenge (Fig. 1g, h). Similar changes were observed in primary BV2 and microglial cells via IF staining (Fig. S1b–S1c). These results suggest that microglial OTUD1 is associated with AD pathology.

OTUD1 deficiency reverses cognitive and synaptic deficits in Aβ-infused mice
To determine the role of OTUD1 in AD-related cognitive dysfunction, we evaluated the learning and memory abilities of OTUD1-deficient mice using the NORT and MWM (Fig. S2a). Aβ injection was used to produce cognitive dysfunction in mice, and NORT was used to record the movement trajectories of mice in each group. $OTUD1^{-/-}$-Aβ group showed increased exploration of novel objects compared to the Aβ group (Fig. 2a–f). In the MWM test, mean escape latency of mice in the $OTUD1^{-/-}$-Aβ group was significantly lower than that of mice in the Aβ group (Fig. 2g–i). After removing the platform, mice in the $OTUD1^{-/-}$-Aβ group crossed the platform and stayed in the target quadrant longer than those in the Aβ group (Fig. 2j, k). These behavioral tests showed that OTUD1 knockout significantly attenuated Aβ-induced cognitive dysfunction in mice. Synaptic changes are closely associated with learning and memory; therefore we examined the protein levels of two key molecules involved in synaptic plasticity and function: neurite cytoskeletal

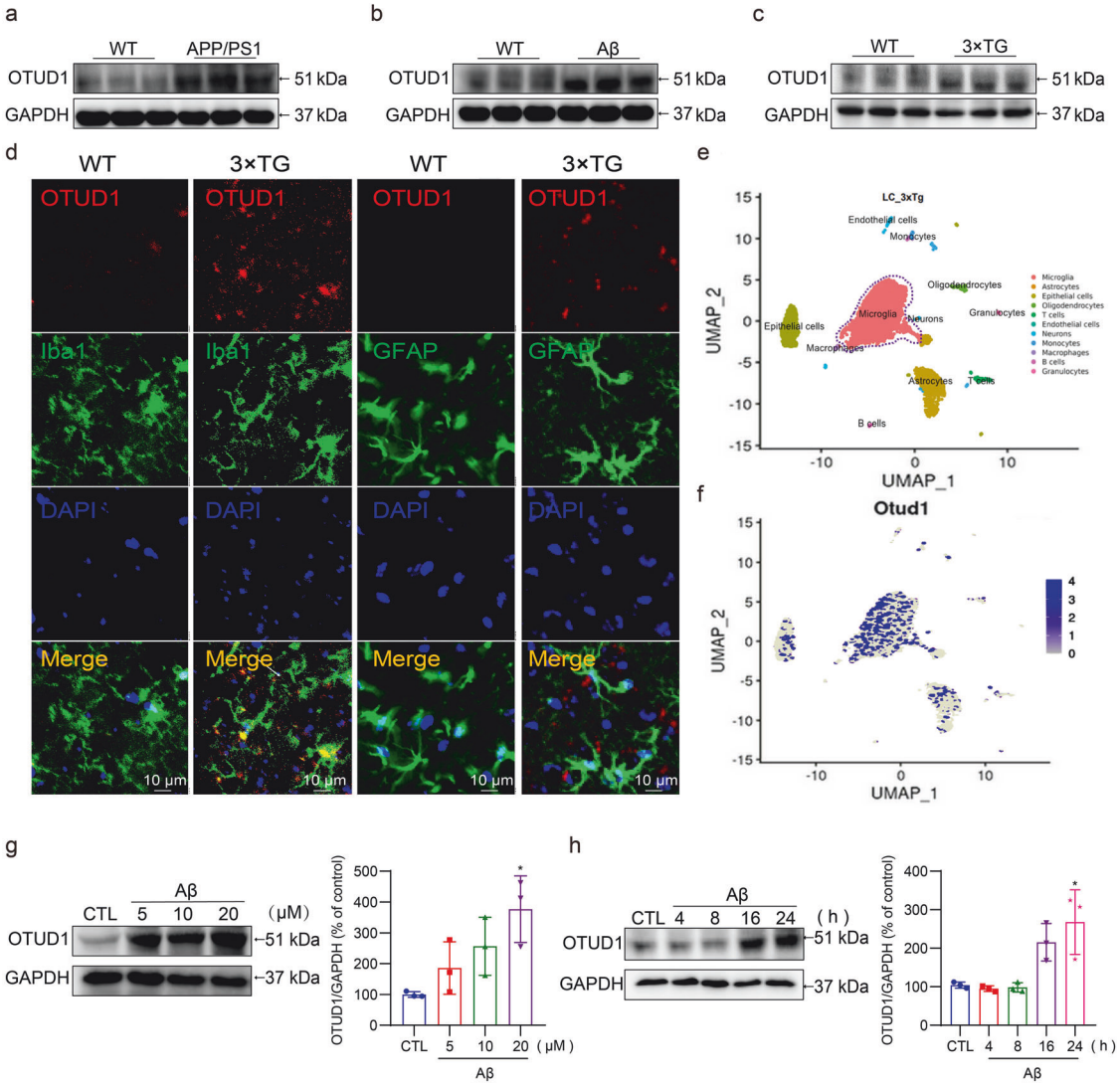

Fig. 1 OTUD1 is upregulated in different AD model mice and Aβ-induced BV2 cells. a Western blot analysis of OTUD1 protein in the hippocampus of 8-month-old APP/PS1 mice and age-matched WT mice. **b** Western blot analysis of OTUD1 protein in the hippocampus of Aβ-infusion mice and age-matched C57BL/6 mice. **c** Western blot analysis of OTUD1 protein in the hippocampus of 8-month-old 3×Tg and age-matched WT mice. **d** Co-staining of microglial marker Iba1 (green) or astrocyte marker GFAP (green) with OTUD1 (red) in the hippocampus of 8-month-old 3×Tg mice and age-matched WT mice (scale bar = 50 μm). **e** A total of 11 cell groups were identified through analysis of brain cell marker genes in single-cell sequencing. **f** Expression analysis of OTUD1 in brain tissue. **g** Representative Western blot bands of OTUD1 in BV2 cells after treatment with Aβ at different concentrations for 24 h. **h** Representative Western blot bands of OTUD1 in BV2 cells after incubation of 20 μM Aβ at different time points. ($n = 3$ independent experiments; Mean ± SEM; $^*P < 0.05$).

microtubule-associated protein 2 (MAP2) and postsynaptic density protein 95 (PSD95). Western blotting showed that OTUD1 deficiency reversed MAP2 and PSD95 level reduction in Aβ-challenged mouse hippocampus (Fig. 2l, m). Compared to that in the Aβ group, dendritic spines density in the hippocampus was increased in OTUD1$^{-/-}$-Aβ group(Fig. S2b, c). IF staining of the mouse hippocampus showed a significant loss of synapses in the Aβ group, while the number of MAP2-expressing cells in the OTUD1$^{-/-}$-Aβ group was significantly increased (Figs. S2d–e). Taken together, these results suggest that OTUD1 deficiency improves cognitive impairment, restores the hippocampal synaptic plasticity, and reverses synaptic injury in Aβ-infused mice.

OTUD1 deficiency reduces neuroinflammation in Aβ-infused mice

To further identify whether OTUD1 deficiency reduces neuroinflammation in microglia, we measured the expression of inflammatory markers in the mouse brain. First, we analyzed the activation of microglia by detecting the level of Iba1 and found that Aβ-infused OTUD1$^{-/-}$ mice showed suppressed microglia activation compared with the Aβ-infused WT mice (Fig. 3a, b and Fig. S2f). Activated microglia are the major source of inflammatory cytokines in the brain. As expected, OTUD1 deletion significantly inhibited the releases of TNF-α and IL-1β induced by Aβ infusion in the mouse hippocampus (Fig. 3c and S2g), suggesting that OTUD1 deficiency reduces Aβ-induced neuroinflammation. In addition, inflammatory cytokines released from the activated microglia further led to neuronal apoptosis. Indeed, Aβ challenge induced the apoptosis-related proteins, Bax/Bcl2 and cleaved caspase 3, and increased neuronal nuclei (NeuN)+ positive cells in the hippocampus, whereas OTUD1 knockout reversed these changes (Fig. 3d, e and S2h). In summary, these results suggest that OTUD1 deficiency reduces neuroinflammation in Aβ-infused mouse hippocampus.

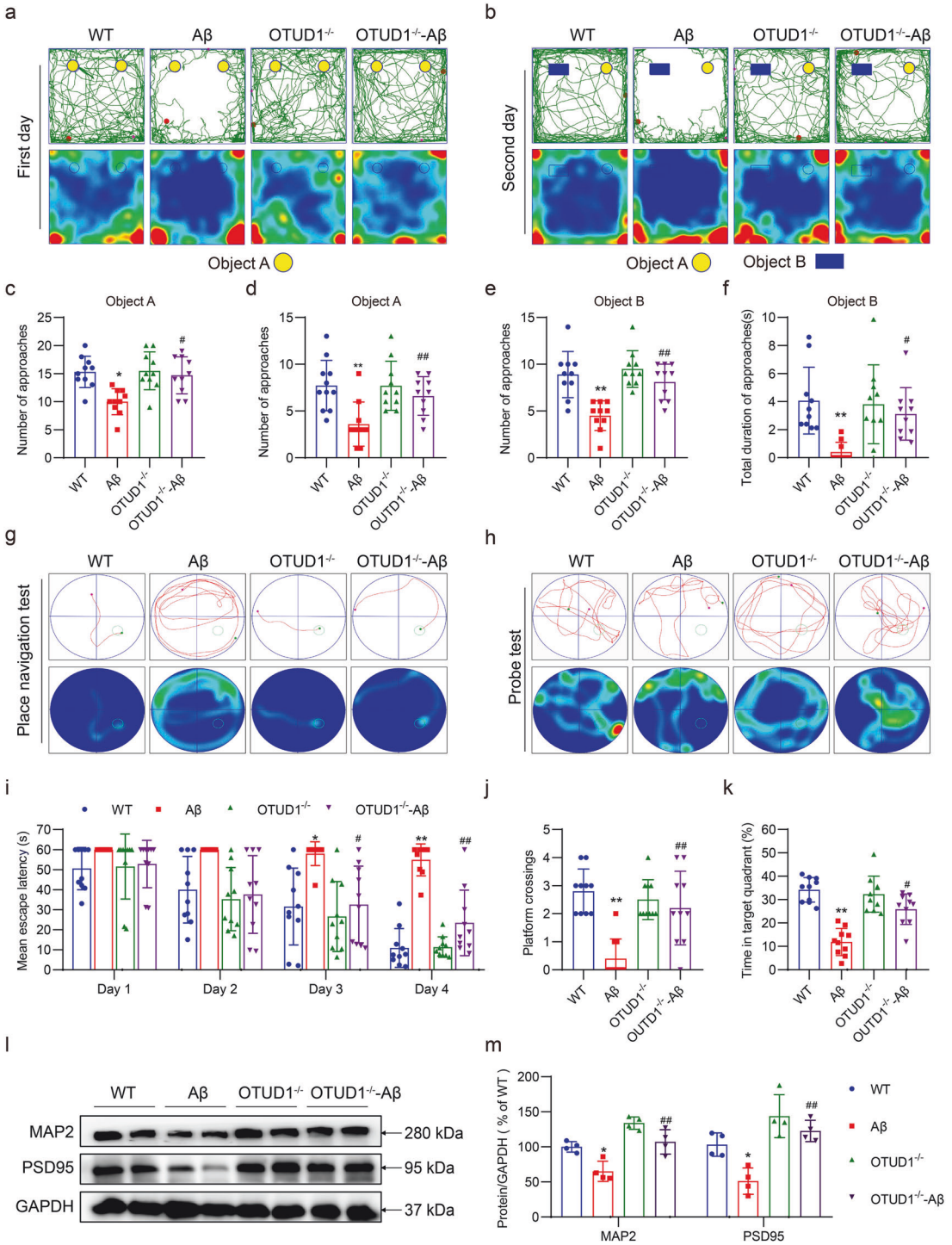

Fig. 2 OTUD1 knockout improves cognitive disfunction and synaptic impairment in Aβ model mice. a Representative movement trajectories of mice in the first day of the NORT. **b** Representative movement trajectories of mice in the second day of the NORT. **c** The total number of approaches to object A on the first day of the NORT. **d** The number of approaches to object A on the second day of the NORT. **e** The number of approaches to object B on the second day of the NORT. **f** Time at which the four groups of mice touched the novel object B on the second day of NORT. **g** Representative swimming trajectories of mice on the fourth day of the MWM. **h** Representative swimming trajectories of mice after hidden platform removal on the fifth day of MWM. **i** Time required for mice to find the hidden platform on the d 1–4 of MWM. **j** After the hidden platform was removed, the number of times in each group of mice passed through the platform area within 60 s. **k** The time that the mice stayed in the target quadrant after the hidden platform was removed on the fifth day of the MWM ($n = 10$ mice/group for A-K panels). **l**, **m** Western blot analysis of MAP2 and PSD95 in the hippocampus of WT, Aβ, OTUD1$^{-/-}$ and OTUD1$^{-/-}$-Aβ ($n = 3$ independent experiments). (Mean ± SEM; $^{*}P < 0.05$ or $^{**}P < 0.01$ versus the WT group; $^{\#}P < 0.05$ or $^{\#\#}P < 0.01$ versus the Aβ group).

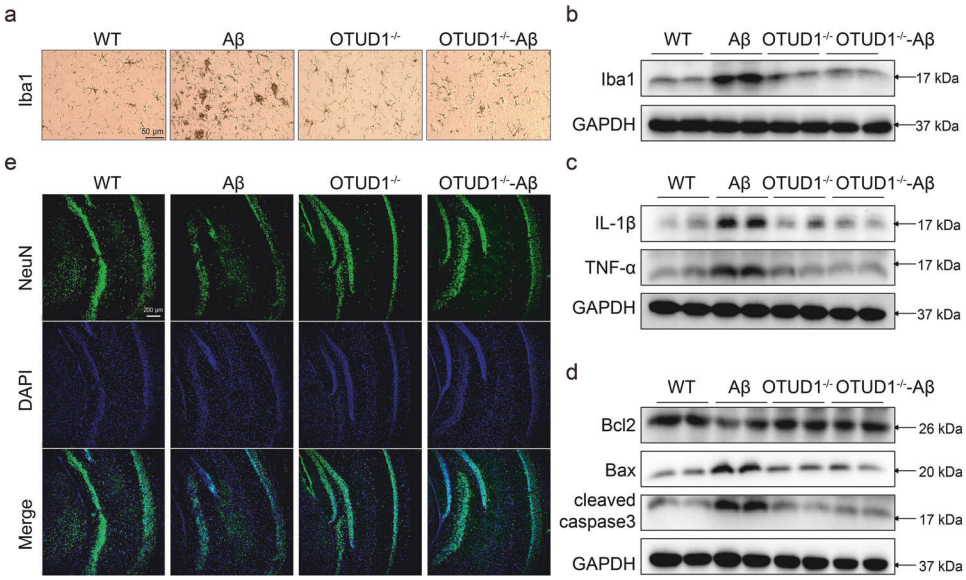

Fig. 3 OTUD1 knockdown improves neuroinflammation in Aβ infused mice. a IHC staining for Iba1 (brown) in the hippocampus of mice (scale bar = 50 μm). **b** Representative Western blot analysis of Iba1 in hippocampal tissue lysates of mice. **c** Representative Western blot analysis of IL-1β and TNF-α in hippocampal tissue lysates of mice. **d** Representative Western blot analysis of Bax, Bcl2, and cleaved caspase3 in hippocampal tissue lysates of mice. **e** Brain sections stained with neuronal nuclei (NeuN; scale bar = 200 μm; $n = 3$ independent experiments).

Microglia-specific knockdown of OTUD1 reverses cognitive deficits in AD mice

To further confirm the role of microglia OTUD1 in AD, we used an adeno-associated virus (AAV) carrying a microglia-specific CX3CR1 promoter to specifically deliver OTUD1 siRNA into mouse microglia. AAV-shOTUD1 was injected into the hippocampus bilaterally in 3×Tg mouse brains to knockdown OTUD1 in microglia, as confirmed via IF (Figs. S3a, b). The 3×Tg mice are among the most widely used animal models of spontaneous AD, with pathologicals, phenotypes such as amyloid plaques, neuroinflammation, and cognitive impairment. We performed behavioral tests including NORT and MWM, on these mice after AAV injection. The results from NORT showed that microglia-specific OTUD1 knockdown significantly increased the total numbers of 3×Tg mice finding both old object and new object (Fig. 4a–f). The MWM results also showed that OTUD1 knockdown in microglia decreased the average time taken by 3×Tg mice to find the hidden platform (Fig. 4g–i). After removing the platform, microglial OTUD1-deficient 3×Tg mice crossed the hidden platform more times (Fig. 4j) and remained in the target quadrant longer than the 3×Tg mice (Fig. 4k). Western blotting analysis showed that the synaptic-related protein MAP2 and PSD95 levels in 3×Tg mice were significantly increased by AAV-shOTUD1 injection (Fig. 4l, m), indicating an improvement in synaptic plasticity. We also evaluated the neuroinflammation in these mice and found that OTUD1 deficiency in microglia significantly improved microglia activation and inflammatory factor release (Figs. S4a–g) and reversed neuronal apoptosis in 3×Tg mice (Figs. S4h,i). Overall, microglia-specific OTUD1 knockdown significantly improves cognitive impairment and neuroinflammation in 3×Tg mice.

OTUD1 positively regulates inflammation in microglia

BV2 cells were used to confirm the role of OTUD1 in regulating inflammation. OTUD1 expression was silenced using OTUD1 siRNA (siOTUD1) (Fig. S5a-S5b). Result from ELISA showed that OTUD1 deficiency reduced the release of the inflammatory cytokine TNF-α (Fig. 5a). Real-time qPCR assay showed that OTUD1 deficiency reduced the mRNA levels of inflammatory genes (Fig. 5b). In contrast, overexpression of OTUD1 in BV2 cells (Fig. S5cd) was found to exacerbate microglial inflammation (Fig. 5c, d). Microglia-derived inflammatory cytokines possibly play key roles in AD pathogenesis by inducing neuronal cell injuries [16]. To evaluate the effects of microglia-derived inflammatory factors on neuronal cells, we collected conditioned media from BV2 cells in different treatment groups (Fig. 5e). The conditioned medium of Aβ-treated BV2 cells increased the apoptosis of PC12 cells, whereas that of OTUD1-deficient BV2 cells failed to damage the PC12 cells (Fig. 5f, g). Indeed, culture medium from OTUD1-overexpressing BV2 cells aggravated the damage of PC12 cells (Fig. 5h, i). Taken together, these results indicate that OTUD1 positively regulates inflammation in microglial cells and then induces neuronal cell damage.

OTUD1 directly interacts with C/EBPβ and up-regulates C/EBPβ stability to promote inflammation in microglia

To determine the underlying molecular mechanisms of microglia OTUD1, we characterized proteins that directly interact with OTUD1 via LC-MS/MS analysis (Fig. 6a). Among potential OTUD1-binding proteins, C/EBPβ, a member of the C/EBP family, aroused our interest (Fig. 6b), as C/EBPβ plays a key role in regulating microglia-mediated neuroinflammation [20]. Co-IP assays confirmed the combination of endogenous OTUD1 and C/EBPβ in hippocampus tissues of Aβ-injected mice (Fig. 6c) and Aβ-challenged BV2 cells (Fig. 6d). Using NIH3T3 tool cells transfected with both OTUD1 and C/EBPβ plasmids, we further validated the exogenous OTUD1-C/EBPβ interation (Fig. 6e). C/EBPβ has three domains: transactivation domain (TAD), regulatory domain (RD), and basic leucine zipper (bZIP) [21, 22]. We constructed 3 mutants of C/EBPβ (Fig. 6f) and co-transfected Flag-OTUD1 and mutant His-C/EBPβ plasmids into NIH3T3 cells, respectively. We found that OTUD1 failed to bind to C/EBPβ when RD is deleted, indicating that OTUD1 binds to the regulatory domain of C/EBPβ (Fig. 6g).

We further explored if OTUD1-C/EBPβ interaction effected C/EBPβ stability or function. Knockdown of OTUD1 in BV2 cells reduced C/EBPβ protein levels, whereas overexpression of OTUD1 increased C/EBPβ protein levels (Fig. 7a, b). Similarly, C/EBPβ protein levels in hippocampal tissue of OTUD1 knockout mice injected with Aβ were significantly lower than that in Aβ-infused WT mice (Fig. 7c). The results were further confirmed in 3×Tg mice injected with AAV-shOTUD1 (Fig. 7d). These data

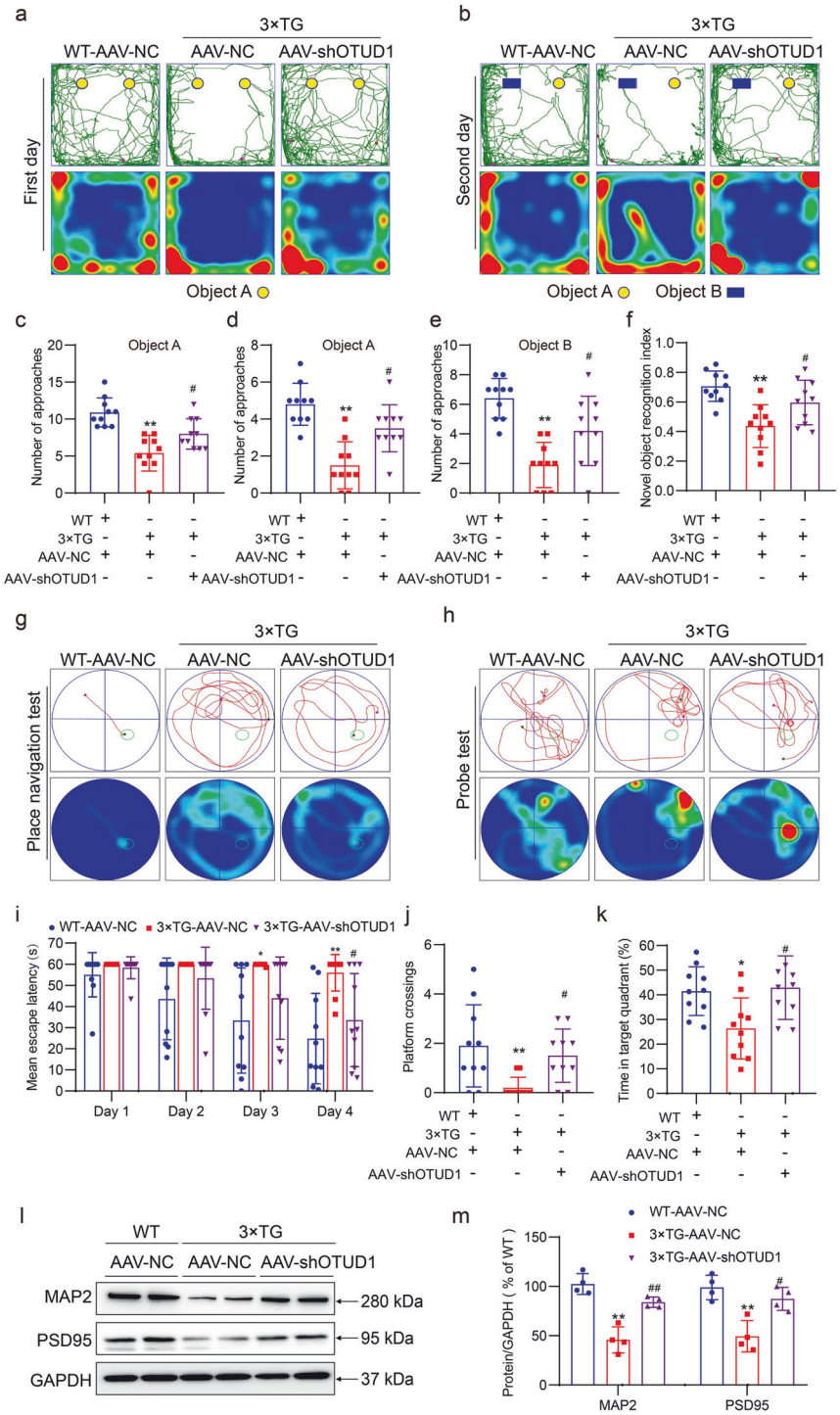

Fig. 4 Microglia OTUD1 knockdown improves cognitive impairment and synaptic function in 3×Tg model mice. a Representative movement trajectories on the first day of NORT. **b** Representative movement trajectories on the second day of NORT. **c** The total number of approaches to object A on the first day of the NORT. **d** The number of approaches to old object A by mice on the second day of NORT. **e** The number of approaches to new object B by mice on the second day of the NORT. **f** Statistical histogram of the Novel object recognition index. **g** Representative trajectories on the fourth day of the MWM. **h** After removing the hidden platform, the representative trajectory of the mice on the fifth day of the MWMT. **i** Time required for mice to find the hidden platform on the d1-4 of the MWM. **j** After the hidden platform was removed, the number of times in each group of mice across the platform area was within 60 s. **k** The time spent in the target quadrant on the fifth day of the MWM ($n = 10$ mice/group for A-J panels). **l** Western blot analysis of MAP2 and PSD95 in the hippocampus of WT-AAV-NC, 3×Tg-AAV-NC, and 3×Tg-AAV-shOTUD1 mice. **m** Quantification analysis of MAP2 and PSD95 in L ($n = 3$ independent experiments for K-L panels). (Mean ± SEM; $^{*}P < 0.05$ or $^{**}P < 0.01$ versus the WT group; $^{\#}P < 0.05$ or $^{\#\#}P < 0.01$ versus the Aβ group).

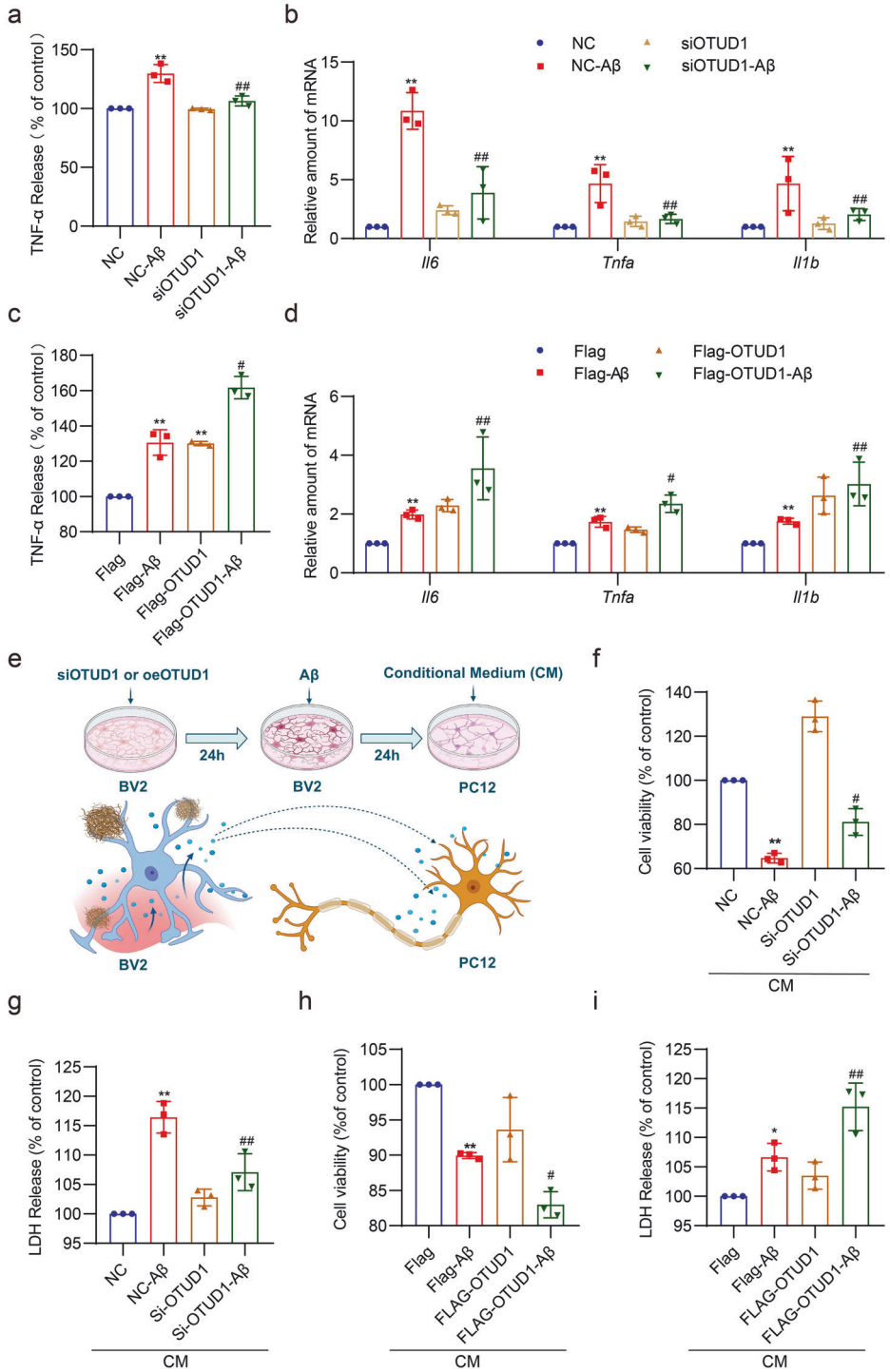

Fig. 5 Microglia OTUD1 inhibition reduces Aβ-induced inflammation and neuronal cell damage. a BV2 cells transfected with siOTUD1 were exposed to 20 μM Aβ for 24 h, and TNF-α release was measured by ELISA assay. **b** RT-qPCR was used to determine the mRNA levels of *Il6*, *Il1b*, and *Tnfa*. **c** BV2 cells transfected with Flag-OTUD1 were exposed to 20 μM Aβ for 24 h, and TNF-α release was measured via ELISA assay. **d** RT-qPCR was used to determine the mRNA levels of *Il6*, *Il1b*, and *Tnfa* in BV2 cells. **e** BV2 cells transfected with siOTUD1 or Flag-OTUD1 were stimulated with/without 20 μM Aβ for an additional 24 h, and conditioned culture supernatants were collected. **f** PC12 cells were divided into four groups: NC, NC-Aβ, siOTUD1, and siOTUD1-Aβ; BV2 serum was added to stimulate PC12 cells for 24 h. Cell viability was determined by the MTT assay. **g** The LDH assay was used to detect cell membrane damage. **h** PC12 cells were divided into four groups: Flag, Flag-Aβ, Flag-OTUD1, and Flag-OTUD1-Aβ; BV2 serum was added to stimulate PC12 cells for 24 h. Cell viability was determined by the MTT assay. **i** Cell membrane damage was tested by LDH assay. ($n = 3$ independent experiments; mean ± SEM; $^{*}P < 0.05$ and $^{**}P < 0.01$ vs. NC or Flag group; $^{\#}P < 0.05$ and $^{\#\#}P < 0.01$ vs. NC-Aβ or Flag-Aβ group).

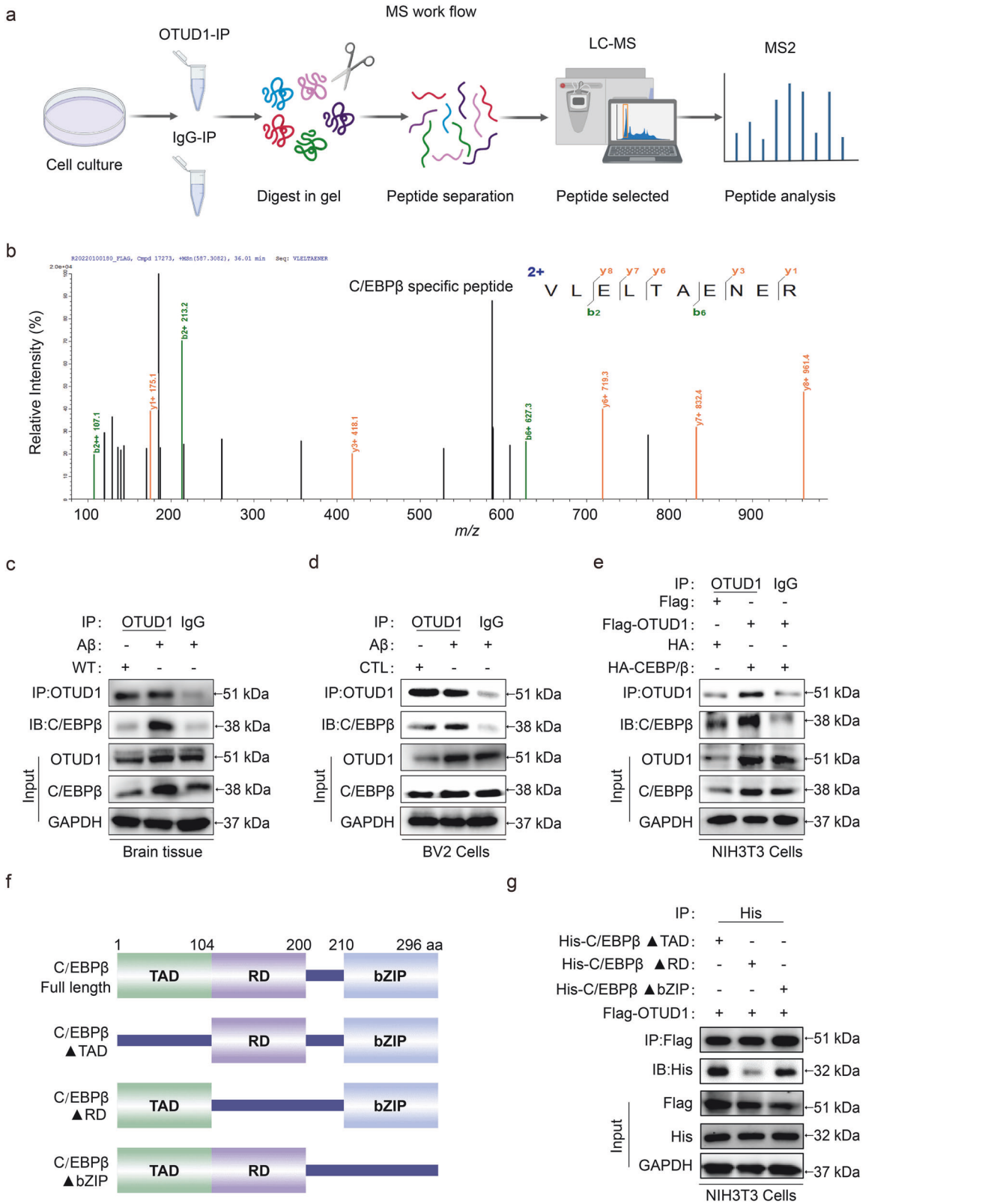

Fig. 6 OTUD1 directly interacts with C/EBPβ. a Schematic illustration of the quantitative proteomic screen to identify proteins binding to OTUD1. **b** MS/MS spectrum of the peptide showing VLELTAENER from C/EBPβ. **c** Co-IP analysis of OTUD1 and C/EBPβ in the hippocampus of mice infused with or without Aβ. **d** Co-IP analysis of OTUD1 and C/EBPβ in microglia induced with or without Aβ. **e** Co-IP analysis of OTUD1 and C/EBPβ in NIH3T3 cells co-transfected with Flag-OTUD1 and HA-C/EBPβ plasmids. **f** Schematic representation of the C/EBPβ domain deletion construct used in **g**. **g** Co-IP analysis of OTUD1 and C/EBPβ in NIH3T3 cells co-transfected with Flag-OTUD1 and His-C/EBPβ, Flag-OTUD1 and His-C/EBPβ ΔTAD, Flag-OTUD1 and His-C/EBPβ ΔRD, Flag-OTUD1 and His-C/EBPβ ΔbZIP. C/EBPβ was detected by Western blot using a Flag antibody. ($n = 3$ independent experiments).

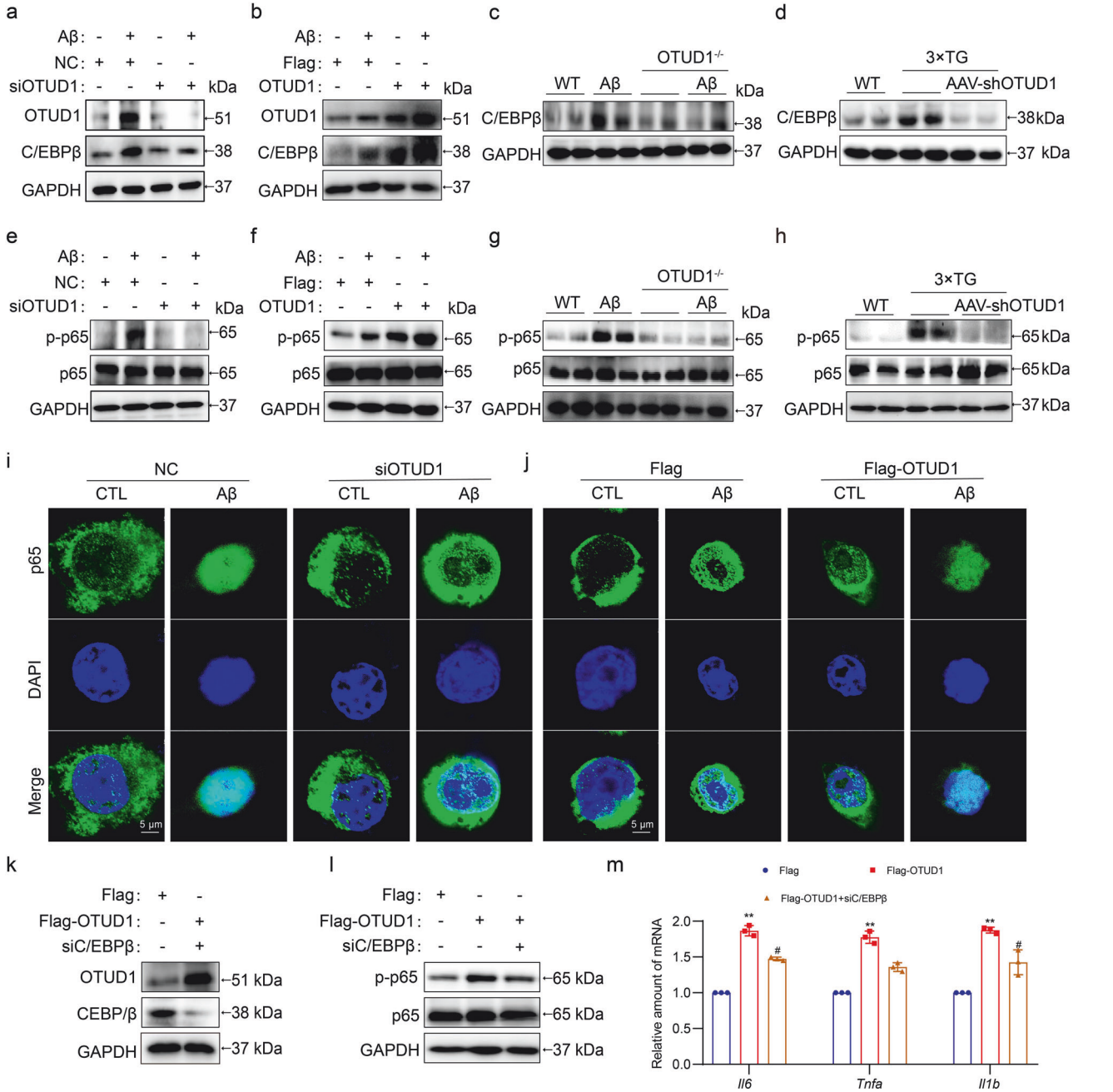

Fig. 7 OTUD1 regulates the stability of C/EBPβ. a BV2 cells transfected with OTUD1 siRNA were exposed to 20 μM Aβ for 24 h, and C/EBPβ and OTUD1 were detected by Western blot. **b** BV2 cells transfected with Flag-OTUD1 overexpression plasmid were stimulated with 20 μM Aβ for 24 h, and C/EBPβ and OTUD1 levels were determined via Western blot. **c** Western blot analysis of C/EBPβ and OTUD1 in the hippocampus of WT, Aβ, OTUD1$^{-/-}$, and OTUD1$^{-/-}$-Aβ mice. **d** Western blot analysis of C/EBPβ and OTUD1 in the hippocampus of WT-AAV-NC, 3×Tg-AAV-NC, and 3×Tg-AAV-shOTUD1 mice. **e** BV2 cells transfected with OTUD1 siRNA and stimulated by Aβ. p65 and p-p65 levels were determined via Western blot. **f** BV2 cells were transfected with OTUD1 overexpression plasmid and stimulated with Aβ. p65 and p-p65 levels were detected by Western blot. **g** Western blot analysis of p65 and p-p65 in the hippocampus of WT, Aβ, OTUD1$^{-/-}$ and OTUD1$^{-/-}$-Aβ mice. **h** Western blot analysis of p65 and p-p65 in the hippocampus of WT-AAV-NC, 3×Tg-AAV-NC, and 3×Tg-AAV-shOTUD1 mice. **i** BV2 cells transfected with OTUD1 siRNA were stimulated with Aβ for 2 h. ICC was used to detect the nuclear import of p65. (scale bar = 5 μm). **j** BV2 cells transfected with Flag-OTUD1 were stimulated with Aβ for 2 h. ICC was used to detect the nuclear import of p65 (scale bar = 5 μm). **k** The overexpression efficiency of OTUD1 and the knockdown efficiency of C/EBPβ were measured by Western blot. **l** The expression levels of p65 and p-p65 were determined by Western blot. **m** RT-qPCR was used to detect the mRNA levels of *Il6*, *Il1b*, and *Tnfa* in BV2 cells. ($n = 3$ independent experiments; mean ± SEM; $^{**}P < 0.01$ vs. Flag group; $^{\#}P < 0.05$ vs. Flag-OTUD1 group).

suggest that OTUD1 positively regulates C/EBPβ protein stability in microglia. It has been reported that C/EBPβ activates NF-κB p65 to induces the expression of inflammatory factor expressions in microglia [23]. Therefore, we examined the effects of OTUD1 on p65 phosphorylation and nuclear translocation. As expected, the phosphorylation of p65 was reduced by OTUD1 knockdown, while overexpression of OTUD1 increased the p65 phosphorylation in Aβ-challenged BV2 cells (Fig. 7e, f). Similar results were confirmed in Aβ infusion model and 3×Tg model mice (Fig. 7g, h). Furthermore, OTUD1 knockdown prevented the

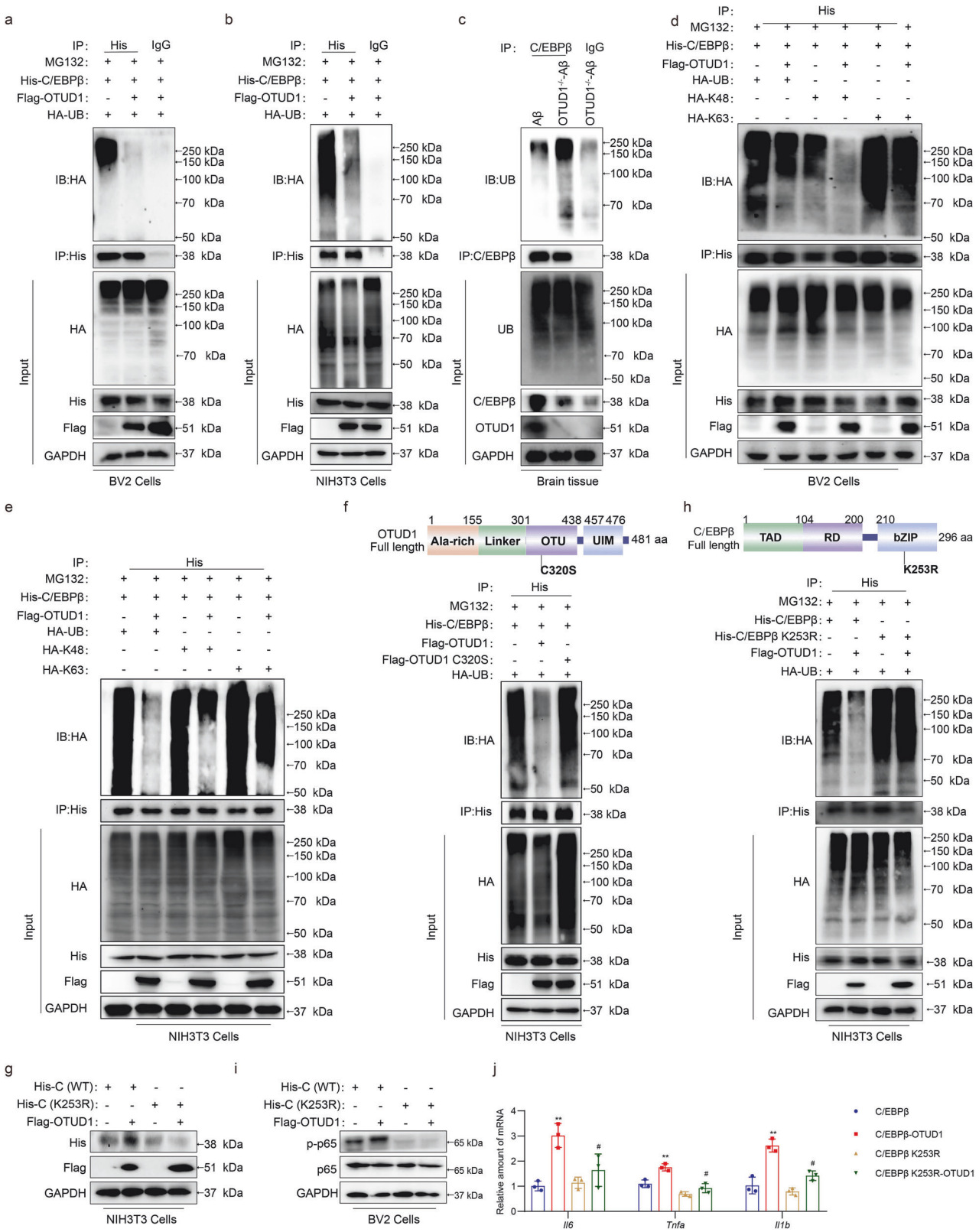

nuclear translocation of p65, while OTUD1 overexpression exacerbated it in Aβ-challenged BV2 cells (Fig. 7i, j and Fig. S6). To further verify that OTUD1 regulates inflammation through C/EBPβ, we used silenced C/EBPβ in BV2 cells overexpressing OTUD1 (Fig. 7k). OTUD1 overexpression-induced p65 phosphorylation and inflammatory gene transcription were significantly reversed by C/EBPβ knockdown (Fig. 7l, m). Taken together, these results suggest that OTUD1 positively regulates inflammation by directly binding to C/EBPβ and enhancing C/EBPβ stability in microglia.

Fig. 8 OTUD1 regulates the expression of C/EBPβ through deubiquitination. a BV2 cells co-transfected with His-C/EBPβ, HA-UB, and Flag-OTUD1 were exposed to MG132 for 6 h, and ubiquitinated C/EBPβ levels were determined via Western blot using a His-specific antibody. **b** NIH3T3 cells co-transfected with His-C/EBPβ, HA-UB, and Flag-OTUD1 were exposed to MG132 for 6 h, and ubiquitinated C/EBPβ levels were determined via Western blot using a His-specific antibody. **c** Brain tissue lysates from OTUD1$^{-/-}$ mice infused with or without Aβ were immunoprecipitated with anti-C/EBPβ, and UB levels were determined via Western blot. **d** BV2 cells co-transfected with His-C/EBPβ, HA-UB, HA-K48, HA-K63, and Flag-OTUD1 were exposed to MG132 for 6 h, ubiquitinated C/EBPβ levels were determined via Western blot using a His-specific antibody. **e** NIH3T3 cells co-transfected with His-C/EBPβ, HA-UB, HA-K48, HA-K63, and Flag-OTUD1 were exposed to MG132, ubiquitinated C/EBPβ levels were determined via Western blot using a His-specific antibody. **f** Schematic illustration of OTUD1 active site deletion construct. NIH3T3 cells co-transfected with His-C/EBPβ, HA-UB, Flag-OTUD1, and Flag-OTUD1C320S were exposed to MG132 for 6 h, ubiquitinated C/EBPβ levels were determined via Western blot using a His-specific antibody. **g** Schematic of the C/EBPβ ubiquitinated lysine residue variant (K253R) construct. NIH3T3 cells co-transfected with His-C/EBPβ, His-C/EBPβ K253R, HA-UB, and Flag-OTUD1 were exposed to MG132 for 6 h, then ubiquitinated C/EBPβ levels were determined via Western blot using a His-specific antibody. **h** Representative immunoblots of OTUD1 and C/EBPβ in NIH3T3 cells co-transfected with Flag-OTUD1, His-C/EBPβ and His-C/EBPβ K253R. **i** Representative immunoblots of p-p65 and p65 in BV2 cells co-transfected with Flag-OTUD1, His-C/EBPβ and His-C/EBPβ K253R. **j** RT-qPCR was used to determine the mRNA levels of *Il6*, *Il1b*, and *Tnfa* in BV2 cells. ($n = 3$ independent experiments; mean ± SEM; $^{**}P < 0.01$ vs. C/EBPβ group; $^{\#}P < 0.05$ vs. C/EBPβ-OTUD1 group).

OTUD1 regulates K48-linked deubiquitination of C/EBPβ at K253 via its active site cysteine 320

To further verify whether OTUD1 enhances C/EBPβ stability via deubiquitination, we co-transfected Flag-OTUD1, His-C/EBPβ, and HA-UB plasmids into BV2 and NIH3T3 cells. OTUD1 reduced the ubiquitination of C/EBPβ (Fig. 8a, b). Similarly, OTUD1 deficiency increased the ubiquitination of C/EBPβ in the mouse hippocampus (Fig. 8c). K48- and K63-linked ubiquitination are the most classic types of ubiquitination modifications [24]. We showed that OTUD1 deubiquitinated C/EBPβ in a K48-linked manner in both BV2 cells and NIH3T3 cells (Fig. 8d, e). Cysteine at position 320 in OTUD1 is the active site for its deubiquitination activity [8, 11]. We constructed an OTUD1 plasmid with a cysteine 320 to serine mutation (C320S). C320S mutation of OTUD1 did not remove the ubiquitin molecules from C/EBPβ (Fig. 8f). Next, we predicted the ubiquitinated lysine residues of C/EBPβ through the websites (GPS-Uber, http://gpsuber.biocuckoo.cn/index.php; UbiqSite, http://systbio.cau.edu.cn/ubiqsite/index.php), and the K253 site have the highest predicted score (Fig. S7). Therefore, we constructed the K253R variant plasmid of C/EBPβ (replacing lysine with arginine at position 253). As shown in Fig. 8g, OTUD1 failed to regulate the stability of C/EBPβ K253R mutant. Furthermore, the ubiquitination level of C/EBPβ-K253R in NIH3T3 cells cannot be reduced by OTUD1 (Fig. 8h). Similarly, OTUD1 could not promote p65 phosphorylation and inflammatory gene expression in BV2 cells with C/EBPβ K253R mutation (Fig. 8i, j). Taken together, these results suggest that OTUD1 promotes K48-linked deubiquitination at K253 through its active site C320, thereby up-regulating C/EBPβ stability and inflammatory response.

DISCUSSION

In this study, OTUD1 levels were up-regulated in different AD model mice, and OTUD1 was mainly expressed in microglia. Both global OTUD1 knockout and specific knockdown of microglial OTUD1 significantly alleviated neuroinflammation and AD pathology in mice. Through mass spectrometry combined with Co-IP analysis, C/EBPβ was identified as a key substrate of OTUD1 in microglia. Mechanistically, OTUD1 deubiquitinates C/EBPβ at K253 in a K48-linked manner through its active site C320, resulting in the reduced degradation of C/EBPβ and the enhanced protein level of C/EBPβ, which activates NF-κB p65-mediated inflammation in microglia. Our data suggest targeting microglial OTUD1 as a potential therapeutic strategy for AD.

Recently, several DUBs have emerged as key neuroinflammation regulators [25, 26]. For example, USP25 alleviates neuroinflammation and rescues synaptic and cognitive functions in AD model mice [27]. USP7 inhibition attenuates microglial activation and neuronal damage, significantly ameliorating behavioral deficits in dementia models [28]. USP19 regulates microglial M1/M2 polarization by deubiquitinating FOXO1 to activate inflammatory signaling. USP18 is a key negative regulator of microglial activation that exerts protective effects on microglial function by regulating the interferon pathway. DUBs are involved in inflammatory AD pathogenesis. OTUD1 regulates the inflammatory responses in different diseases and conditions [29], including hypertension-induced kidney and heart damage [11, 12], viral infections [7], colitis [8], and periodontitis [29]. OTUD1 is also been associated with innate immune diseases and cancer [10, 30]. In AD, neuroinflammation is mainly mediated by microglia [31, 32], and downregulating the inflammatory responses of microglia is beneficial for AD treatment. In this study, OTUD1 was mainly expressed in microglia, and the knockdown of microglial OTUD1 in AD model mice reduced the inflammatory responses and improved cognitive impairment. A limitation of this study is that we did not use microglia-specific OTUD1 knockout 3xTG mice to elucidate the roles of OTUD1 in AD. Nevertheless, we specifically knocked down microglial OTUD1 in 3×Tg mice by injecting AAV into the hippocampus of 3×Tg mice, which supports our conclusions.

DUBs exert their effects and functions mainly by binding to their substrates. For example, A20 regulates the NF-κB signaling pathway and neuroinflammation by deubiquitinating TRAF6 [33, 34]. USP25 deficiency reverses neuroinflammation in AD model mice by targeting WDFY1 and ATP6V0C [27]. USP11 activates the NF-κB inflammatory signaling pathway by deubiquitinating p53 [35]. In this study, OTUD1 directly bound to C/EBPβ and increased its protein stability. C/EBPβ is a key protein regulating microglial activation [23, 36]. Cebpb transcript (encoding C/EBPβ) is more abundant in the brains of aged AD model mice than in those of aged WT mice [37]. Reduction in C/EBPβ levels improves Tau pathology and cognitive dysfunction in AD model mice [38]. Natural products that inhibit C/EBPβ expression have significantly improved AD pathology. For example, patchouli alcohol inhibits neuroinflammation and improves cognitive deficits in AD model mice by inhibiting the activation of the C/EBPβ/AEP pathway [39]. Troxerutin alleviates memory deficits in mice by inhibiting C/EBPβ-mediated inflammatory responses [40]. Inhibition of C/EBPβ-NFκB p65 interaction by carnosic acid ameliorates neuroinflammation and improves cognitive function in AD models [23]. However, these natural inhibitors lack specificity in inhibiting C/EBPβ, and small-molecule inhibitors specifically targeting C/EBPβ have not yet been identified. Here, OTUD1 knockout reduced the C/EBPβ levels in microglia, thereby alleviating the inflammatory responses and AD pathology. Therefore, targeting OTUD1 is a potential strategy to treat AD by reducing C/EBPβ levels.

Both C/EBPβ stability and activity are regulated by post-translational ubiquitinating modifications [41]. E3 ubiquitin ligases regulate C/EBPβ in AD. For example, E3 ubiquitin ligase COP1

inhibits neuroinflammation and alleviates Tau-driven AD pathology by regulating C/EBPβ stability in mice [20]. Pellino 1 acts as a direct E3 ubiquitin ligase of C/EBPβ and mediates its ubiquitination to induce C/EBPβ degradation in microglia [42]. E3 ubiquitin ligases Nrdp1 and Mdm2 promote ubiquitination-mediated C/EBPβ degradation [43]. However, only a few DUBs have been reported to deubiquitinate C/EBPs. To date, only USP1 has been found to enhance the stability of C/EBPβ by deubiquitinating it, thereby accelerating adipogenesis and lipid accumulation [44]. Here, we identified OTUD1 as a new DUB regulating the deubiquitination and stability of C/EBPβ. OTUD1 removes K48-linked ubiquitin molecules from C/EBPβ via its active site C320. Moreover, the lysine sites involved in ubiquitination modification of C/EBPβ have not been reported. Previous studies have reported that the K134 site on the RD motif of rat C/EBPβ is SUMOylated [45]. Here, we identified a lysine residue (K253) on C/EBPβ as the key site for OTUD1 deubiquitination. Our findings suggest that, deubiquitination at K253 or K253R mutation increases C/EBPβ protein stability in microglia and promotes microglial inflammatory responses and AD pathology, underscoring the important crucial impact of K253 ubiquitination on C/EBPβ protein stability.

In conclusion, our study highlights the critical role of microglial OTUD1 in neuroinflammation and AD pathology, revealing a novel mechanism of the microglial OTUD1–C/EBPβ axis in AD development. Therefore, OTUD1-targeting interventions show potential for AD treatment.

ACKNOWLEDGEMENTS

This study was supported by the Natural Science Foundation of Zhejiang Province (ZCLQN25H3101 to LYS.), National Natural Science Foundation of China (21961142009 to GL), Zhejiang Provincial Key Scientific Project (2021C03041 to GL), and Medical and Health Science and Technology Project of Zhejiang Province (2024KY055 to XZ).

AUTHOR CONTRIBUTIONS

GL and XZ contributed to the literature search and study design. LYS participated in the drafting of the article. LYS, LYL, HT, YQZ, FYG, JFS, LWL, and LX carried out the experiments. FC, QY and LJC contributed to data collection and analysis. WHZ contributes to methodology. GL and XZ revised the manuscript.

ADDITIONAL INFORMATION

Supplementary information The online version contains supplementary material available at https://doi.org/10.1038/s41401-025-01566-y.

Competing interests: The authors declare no competing interests.

REFERENCES

1. 2023 Alzheimer's disease facts and figures. Alzheimers Dement. 2023;19:1598–695.
2. Sharma H, Chang K-A, Hulme J, An SSA. Mammalian models in Alzheimer's research: an update. Cells. 2023;12:2459.
3. Srivastava S, Ahmad R, Khare SK. Alzheimer's disease and its treatment by different approaches: A review. Eur J Med Chem. 2021;216:113320.
4. Ocañas SR, Pham KD, Cox JEJ, Keck AW, Ko S, Ampadu FA, et al. Microglial senescence contributes to female-biased neuroinflammation in the aging mouse hippocampus: implications for Alzheimer's disease. J Neuroinflammation. 2023;20:188.
5. Yang Y, García-Cruzado M, Zeng H, Camprubí-Ferrer L, Bahatyrevich-Kharitonik B, Bachiller S, et al. LPS priming before plaque deposition impedes microglial activation and restrains Aβ pathology in the 5xFAD mouse model of Alzheimer's disease. Brain Behav Immun. 2023;113:228–47.
6. Schaffer Aguzzoli C, Ferreira PCL, Povala G, Ferrari-Souza JP, Bellaver B, Soares Katz C, et al. Neuropsychiatric symptoms and microglial activation in patients with Alzheimer disease. JAMA Netw Open. 2023;6:e2345175.
7. Lin J, Zheng Y, Zhao N, Cui F, Wu S. Herpesvirus latent infection promotes stroke via activating the OTUD1/NF-κB signaling pathway. Aging (Albany NY). 2023;15:8976–92.
8. Oikawa D, Gi M, Kosako H, Shimizu K, Takahashi H, Shiota M, et al. OTUD1 deubiquitinase regulates NF-κB- and KEAP1-mediated inflammatory responses and reactive oxygen species-associated cell death pathways. Cell Death Dis. 2022;13:694.
9. Zhang Z, Wang D, Wang P, Zhao Y, You F. OTUD1 negatively regulates type I IFN induction by disrupting noncanonical ubiquitination of IRF3. J Immunol. 2020;204:1904–18.
10. Lu D, Song J, Sun Y, Qi F, Liu L, Jin Y, et al. Mutations of deubiquitinase OTUD1 are associated with autoimmune disorders. J Autoimmun. 2018;94:156–65.
11. Wang M, Han X, Yu T, Wang M, Luo W, Zou C, et al. OTUD1 promotes pathological cardiac remodeling and heart failure by targeting STAT3 in cardiomyocytes. Theranostics. 2023;13:2263–80.
12. Wang M, Yu T, Wang Q, Han X, Hu X, Ye S, et al. OTUD1 promotes hypertensive kidney fibrosis and injury by deubiquitinating CDK9 in renal epithelial cells. Acta Pharmacol Sin. 2023;45:765–76.
13. Sun J, Li L, Xiong L, Chen F, She L, Tang H, et al. Parthenolide alleviates cognitive dysfunction and neurotoxicity via regulation of AMPK/GSK3β(Ser9)/Nrf2 signaling pathway. Biomed Pharmacother. 2023;169:115909.
14. She L, She L, Sun J, Xiong L, Li A, Li L, et al. Ginsenoside RK1 improves cognitive impairments and pathological changes in Alzheimer's disease via stimulation of the AMPK/Nrf2 signaling pathway. Phytomedicine. 2024;122:155168.
15. Li Y, Zhang ZH, Huang SL, Yue ZB, Yin XS, Feng ZQ, et al. Whey protein powder with milk fat globule membrane attenuates Alzheimer's disease pathology in 3×Tg-AD mice by modulating neuroinflammation through the peroxisome proliferator-activated receptor γ signaling pathway. J Dairy Sci. 2023;106:5253–65.
16. Zhao X, Sun J, Xiong L, She L, Li L, Tang H, et al. β-amyloid binds to microglia Dectin-1 to induce inflammatory response in the pathogenesis of Alzheimer's disease. Int J Biol Sci. 2023;19:3249–65.
17. Huang Z, Shen S, Wang M, Li W, Wu G, Huang W, et al. Mouse endothelial OTUD1 promotes angiotensin II-induced vascular remodeling by deubiquitinating SMAD3. EMBO Rep. 2023;24:e56135.
18. Ali M, Garcia P, Lunkes LP, Sciortino A, Thomas M, Heurtaux T, et al. Single cell transcriptome analysis of the THY-Tau22 mouse model of Alzheimer's disease reveals sex-dependent dysregulations. Cell Death Discov. 2024;10:119.
19. Yan Y, Wang X, Chaput D, Shin MK, Koh Y, Gan L, et al. X-linked ubiquitin-specific peptidase 11 increases tauopathy vulnerability in women. Cell. 2022;185:3913–30.e19.
20. Ndoja A, Reja R, Lee SH, Webster JD, Ngu H, Rose CM, et al. Ubiquitin ligase COP1 suppresses neuroinflammation by degrading c/EBPβ in microglia. Cell. 2020;182:1156–69.e12.
21. Tsukada J, Yoshida Y, Kominato Y, Auron PE. The CCAAT/enhancer (C/EBP) family of basic-leucine zipper (bZIP) transcription factors is a multifaceted highly-regulated system for gene regulation. Cytokine. 2011;54:6–19.
22. Leutz A, Pless O, Lappe M, Dittmar G, Kowenz-Leutz E. Crosstalk between phosphorylation and multi-site arginine/lysine methylation in C/EBPs. Transcription. 2011;2:3–8.
23. Yi-Bin W, Xiang L, Bing Y, Qi Z, Fei-Tong J, Minghong W, et al. Inhibition of the CEBPβ-NFκB interaction by nanocarrier-packaged carnosic acid ameliorates glia-mediated neuroinflammation and improves cognitive function in an Alzheimer's disease model. Cell Death Dis. 2022;13:318.
24. Mikami T, Majima S, Song H, Bode JW. Biocompatible lysine protecting groups for the chemoenzymatic synthesis of K48/K63 heterotypic and branched ubiquitin chains. ACS Cent Sci. 2023;9:1633–41.
25. Hu H, Sun S-C. Ubiquitin signaling in immune responses. Cell Res. 2016;26:457–83.
26. Tanji K, Mori F, Miki Y, Utsumi J, Sasaki H, Kakita A, et al. YOD1 attenuates neurogenic proteotoxicity through its deubiquitinating activity. Neurobiol Dis. 2018;112:14–23.
27. Zheng Q, Li G, Wang S, Zhou Y, Liu K, Gao Y, et al. Trisomy 21–induced dysregulation of microglial homeostasis in Alzheimer's brains is mediated by USP25. Sci Adv. 2021;7:eabe1340.
28. Zhang XW, Feng N, Liu YC, Guo Q, Wang JK, Bai YZ, et al. Neuroinflammation inhibition by small-molecule targeting USP7 noncatalytic domain for neurodegenerative disease therapy. Sci Adv. 2022;8:eabo0789.
29. Song J, Zhang Y, Bai Y, Sun X, Lu Y, Guo Y, et al. The deubiquitinase OTUD1 suppresses secretory neutrophil polarization and ameliorates immunopathology of periodontitis. Adv Sci (Weinh). 2023;10:2303207.
30. Zhang Z, Fan Y, Xie F, Zhou H, Jin K, Shao L, et al. Breast cancer metastasis suppressor OTUD1 deubiquitinates SMAD7. Nat Commun. 2017;8:2116.
31. Gao C, Jiang J, Tan Y, Chen S. Microglia in neurodegenerative diseases: mechanism and potential therapeutic targets. Signal Transduct Target Ther. 2023;8:359.
32. Cheng J, Dong Y, Ma J, Pan R, Liao Y, Kong X, et al. Microglial Calhm2 regulates neuroinflammation and contributes to Alzheimer's disease pathology. Sci Adv. 2021;7:eabe3600.

33. Li Z, Chu S, He W, Zhang Z, Liu J, Cui L, et al. A20 as a novel target for the anti-neuroinflammatory effect of chrysin via inhibition of NF-κB signaling pathway. Brain Behav Immun. 2019;79:228–35.
34. Wang Y, Yang Z, Wang Q, Ren Y, Wang Q, Li Z, et al. Bavachin exerted anti-neuroinflammatory effects by regulation of A20 ubiquitin-editing complex. Int Immunopharmacol. 2021;100:108085.
35. Zhang X, Liu T, Xu S, Gao P, Dong W, Liu W, et al. A pro-inflammatory mediator USP11 enhances the stability of p53 and inhibits KLF2 in intracerebral hemorrhage. Mol Ther Methods Clin Dev. 2021;21:681–92.
36. Fonseca GJ, Seidman JS, Glass CK. Genome-wide approaches to defining macrophage identity and function. Microbiol Spectr. 2016;4:10.
37. Srinivasan K, Friedman BA, Larson JL, Lauffer BE, Goldstein LD, Appling LL, et al. Untangling the brain's neuroinflammatory and neurodegenerative transcriptional responses. Nat Commun. 2016:7:11295.
38. Wang Z-H, Gong K, Liu X, Zhang Z, Sun X, Wei ZZ, et al. C/EBPβ regulates delta-secretase expression and mediates pathogenesis in mouse models of Alzheimer's disease. Nat Commun. 2018;9:1784.
39. Xu QQ, Su ZR, Yang W, Zhong M, Xian YF, Lin ZX, et al. Patchouli alcohol attenuates the cognitive deficits in a transgenic mouse model of Alzheimer's disease via modulating neuropathology and gut microbiota through suppressing C/EBPβ/AEP pathway. J Neuroinflammation. 2023;20:19.
40. Lu J, Wu DM, Zheng YL, Hu B, Cheng W, Zhang ZF, et al. Troxerutin counteracts domoic acid–induced memory deficits in mice by inhibiting CCAAT/enhancer binding protein β–mediated inflammatory response and oxidative stress. J Immunol. 2013;190:3466–79.
41. Ren Q, Liu Z, Wu L, Yin G, Xie X, Kong W, et al. C/EBPβ: The structure, regulation, and its roles in inflammation-related diseases. Biomed Pharmacother. 2023;169:115938.
42. Xu J, Yu T, Pietronigro EC, Yuan J, Arioli J, Pei Y, et al. Peli1 impairs microglial Aβ phagocytosis through promoting C/EBPβ degradation. PLoS Biol. 2020;18:e3000837.
43. Fu D, Lala-Tabbert N, Lee H, Wiper-Bergeron N. Mdm2 promotes myogenesis through the ubiquitination and degradation of CCAAT/enhancer-binding protein β. J Biol Chem. 2015;290:10200–7.
44. Kim MS, Baek JH, Lee J, Sivaraman A, Lee K, Chun KH, et al. Deubiquitinase USP1 enhances CCAAT/enhancer-binding protein beta (C/EBPβ) stability and accelerates adipogenesis and lipid accumulation. Cell Death Dis. 2023;14:776.
45. Wang L, Wang P, Xu S, Li Z, Duan DD, Ye J, et al. The cross-talk between PAR-ylation and SUMOylation in C/EBPβ at K134 site participates in pathological cardiac hypertrophy. Int J Biol Sci. 2022;18:783–99.